A single-molecule blueprint for synthesis

Ilana Stone[1,5], *Rachel L. Starr*[1,5], *Yaping Zang*[2,4], *Colin Nuckolls*[1], *Michael L. Steigerwald*[1], *Tristan H. Lambert*[3], *Xavier Roy*[1] ✉ *and Latha Venkataraman*[1,2] ✉

Abstract | Chemical reactions that occur at nanostructured electrodes have garnered widespread interest because of their potential applications in fields including nanotechnology, green chemistry and fundamental physical organic chemistry. Much of our present understanding of these reactions comes from probes that interrogate ensembles of molecules undergoing various stages of the transformation concurrently. Exquisite control over single-molecule reactivity lets us construct new molecules and further our understanding of nanoscale chemical phenomena. We can study single molecules using instruments such as the scanning tunnelling microscope, which can additionally be part of a mechanically controlled break junction. These are unique tools that can offer a high level of detail. They probe the electronic conductance of individual molecules and catalyse chemical reactions by establishing environments with reactive metal sites on nanoscale electrodes. This Review describes how chemical reactions involving bond cleavage and formation can be triggered at nanoscale electrodes and studied one molecule at a time.

Over the past two decades, the scanning tunnelling microscope (STM) has been transformed from being primarily an imaging instrument to a device capable of manipulating single atoms and molecules in chemical reactions. These are at the heart of single-molecule chemistry and reveal how chemistry can be reimagined outside of conventional bulk synthesis. Yet, instrumental complexities and the requirement for ultra-high vacuum (UHV) and analyte–surface binding limit the scale and scope of these reactions. Thus, they cannot serve as a general replacement for conventional synthesis but, instead, offer detailed fundamental insights into the chemistry at play. In particular, using the STM break junction (STM-BJ) technique, one can reliably and reproducibly measure the conductance of single molecules in solution by attaching them to metal electrodes. Probing transformations in solution environments and developing a molecular-level understanding of the processes might help us design chemical reactions with novel kinetics and modulated thermodynamics. A STM is unique in that it applies a strongly directional electric field to a molecular system. Combining this with external stimuli such as light and pH further broadens the scope of reactions that can be studied using STM under ambient conditions — ambient temperature, pressure and no inert gas. The tools that enable and help us understand these processes are only now converging and most of the work detailed in this Review has been published in the last 5–10 years. As this burgeoning field reaches a tipping point, we contextualize these results within the realms of both single-molecule manipulation and synthetic chemistry to evaluate the accomplishments and future promise of these methods.

Although some of the experiments described here are better known for their implications in molecular electronics, this Review focuses on the chemical transformations at play in this research. In some ways, the chemistry is ancillary to the functionality of molecular devices, yet, these are, nevertheless, groundbreaking transformations that occur in environments that were never intended for chemical reactions. We describe the implications of these transformations for synthetic chemistry.

We pay particular attention to bond cleavage or formation in molecules anchored to nanoelectrodes that exert a local potential. The STM can be used as a tool for reaction chemistry and we describe how to probe solution-phase reactions following different mechanisms and the implications these have for chemical catalysis. These can be contrasted to reactions monitored at the single-molecule level that can only occur in a single-molecule junction.

Our first reactions presented will be those that are catalysed and controlled using the STM. Early examples are restricted to on-surface processes that differ from the solution reactions that can also be studied in a STM. Reactions induced by the STM tip and thermal reactions that are imaged using a STM are considered separately,

[1]*Department of Chemistry, Columbia University, New York, NY, USA.*

[2]*Department of Applied Physics and Applied Mathematics, Columbia University, New York, NY, USA.*

[3]*Department of Chemistry and Chemical Biology, Cornell University, Ithaca, NY, USA.*

[4]*Present address: CAS Key Laboratory of Organic Solids, Institute of Chemistry, Chinese Academy of Sciences, Beijing, China.*

[5]*These authors contributed equally: Ilana Stone, Rachel L. Starr.*

✉*e-mail: xr2114@columbia.edu; lv2117@columbia.edu*

https://doi.org/10.1038/s41570-021-00316-y

and the latter are used to illustrate the capabilities of the STM that cannot be accomplished using break junction techniques. The challenges and limitations of these surface reactions are also considered, and more recent examples of STM-induced reactions illustrate the evolution of STM surface chemistry and its growing scope. These recent studies reveal how surface reactions have inherent limitations that necessitate the development of new and complementary tools such as the break junction. Thus, the remainder and majority of the Review is dedicated to reactions in break junctions triggered by the local potential of the electrodes. Recent examples illustrate how this technique accesses reactivity that is unattainable by either traditional solution chemistry or the manipulation of specific surface adsorbates. We categorized reactions in this section according to their mechanisms and catalytic implications. The in situ formation of Au–C and heterometallic M–M′ covalent bonds are considered from the perspective of organometallic chemistry. Although both strategies obviously rely on electric fields, we distinguish electrochemically gated reactions from electrostatic reactions. Reactions that integrate other modes of catalysis by working in concert with external stimuli such as the application of light and mechanical force are briefly discussed, as they are especially relevant to dual catalysis strategies involving photoredox[1,2] and the emerging field of electrophotocatalysis[3–5].

The last reactions detailed are those in which junction-based techniques precisely impart unique redox activity to one molecule at a time. These reactions are monitored at the single-molecule level and can only occur in a single-molecule junction. The transformation of each molecule in solution can be probed in real time using the STM-BJ; only molecules held between the electrodes undergo the transformation. Although these reactions are less scalable, they demonstrate a level of precision that is unachievable by any other means. Finally, we address the challenges of translating fundamental experiments into practical reactions with an eye towards developing these powerful analytical tools into a template for nanoscale materials synthesis.

STM-driven surface chemistry

Although it was not originally intended as such, a STM can be used as a tool for reaction chemistry. In each of the reactions outlined in this Review, the STM controls the formation and cleavage of chemical bonds to give new chemical species[6–17] or molecular conformations[18–27]. The pioneering work that established the STM tip as a nanocatalyst for chemical reactions involved molecular surface adsorbates under UHV. The metal tips we discuss are typically made of Au, but W, Ni and other metals are also common. In all, these seminal studies combined the ability of the STM to control mechanical motions such as lateral movement and vertical transfer[28–37], with the ability to manipulate molecules electronically. The latter involved either stimulating adsorbates through the tunnelling current[6,7,10–12,16,20,24], the applied electric field between the tip and the molecule[18,19,25–27] or a combination of both mechanisms.

In this section, we describe some of the fundamental achievements that redefined the STM as a tool to control chemistry at the spatial limit of individual atoms and molecules adsorbed on surfaces. This enables us to investigate the properties of individual molecules while simultaneously manipulating their chemical connectivity. The STM is used to induce bond formation one atom at a time and we can observe individual steps of a chemical reaction and characterize the product(s). More recent examples of surface reactions are discussed to illustrate the versatility of the STM to induce and probe reactivity, and to show how mechanisms have been elucidated over the last 20 years.

Foundational reactions

The STM was first introduced as a nanocatalyst for bond formation with the controlled, step-by-step formation of individual Fe(CO) moieties from Fe atoms at the tip and CO molecules adsorbed on Ag(110)[6] (FIG. 1a). This work capitalized on the mechanical precision with which the STM tip locates and translates individual CO molecules. By tuning the tunnelling current in the STM junction, one can induce Fe–CO coordination. The reaction proceeded in a series of mechanical and electrical steps, in which the tunnelling current was used to locate and move CO molecules to available Fe atoms. In the absence of tunnelling current, bond formation does not occur, even when Fe and CO are in close proximity, demonstrating that the electrical environment of the STM between the tip and the surface is necessary to drive the reaction. The conformation of the newly formed Fe–CO bonds was studied by imaging and inelastic electron tunnelling spectroscopy, demonstrating the multidimensional use of the STM to control and observe a stepwise reaction at the single-molecule level.

Shortly after the report of the Fe(CO) complex came the first organic reaction controlled by a STM — Ullmann homocoupling of PhI on Cu(111)[7] (FIG. 1b). The Ullmann coupling is a ubiquitous chemical transformation used widely in organic syntheses to couple aryl units together and form new C–C bonds, starting with simple and readily available aryl halide precursors[38,39]. The Ullmann coupling has been an especially attractive strategy to prepare graphene nanoribbons[40]. Here, the STM tip was used to control each step of the bimolecular reaction: dehalogenation of PhI, diffusion of the newly formed Ph$^{\cdot}$ radical and formation of a new C–C bond. By injecting electrons into single molecules and monitoring changes in conductance due to a dehalogenation event, one finds a linear dependence of the dissociation rate on the tunnelling current, consistent with only a single electron being required to break a C–I bond. They then used the tip–adsorbate forces[32,33] to move the resulting Ph$^{\cdot}$ species to meet a second Ph$^{\cdot}$ and release it from the tip. An inelastic tunnelling bias excited the molecules and initiated C–C bond formation to complete the homocoupling.

Formation of both the Fe–CO moiety and PhPh are fundamental reactions that rely on the mechanical precision of the STM nanoelectrode to pick out individual molecules and establish an electrical field, under an applied bias, to induce reactivity. The Ullmann reaction especially revealed that common and practical synthetic reactions could be studied at the single-molecule

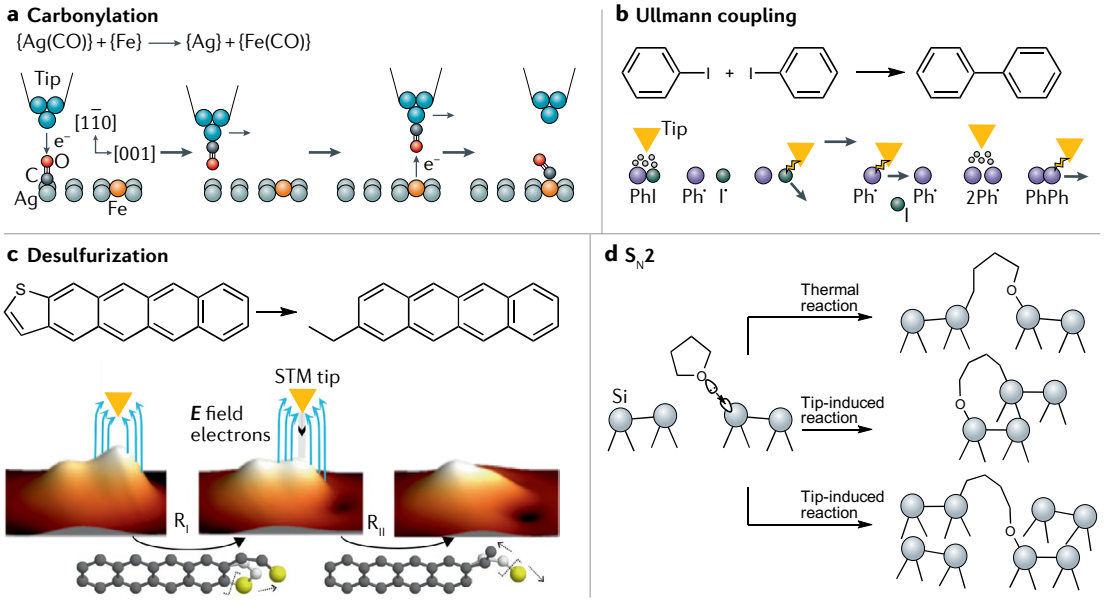

Fig. 1 | **A scanning tunnelling microscope can drive diverse chemical reactions.** Reactions on surfaces rely on the mechanical precision of the scanning tunnelling microscope (STM) nanoelectrode to pick out individual adsorbates and induce reactivity with an applied bias. **a** | The STM is used to control the step-by-step formation of individual Fe(CO) groups on the surface[6]. The tunnelling current can be used to locate and move CO molecules to available Fe atoms, with bond formation only occurring on passing of a tunnelling current. **b** | Ullmann homocoupling of PhI on Cu(111) can be controlled by a STM tip. The bimolecular reaction is induced by injecting electrons into single molecules[7]. The tip can move away the I fragments and drag the Ph groups together. **c** | The STM locally triggers desulfurization of a thiophene subunit of a tetracenothiophene molecule on Cu(111). In the first step, the applied bias leads to one C–S bond cleavage. Then, injection of electrons helps cleave the second C–S bond and realize the exergonic release of S. Alternatively, the reaction can proceed in one single step[9]. **d** | An S_N2 ring-opening reaction of tetrahydrofuran on Si(001). Depending on the bias applied to the STM tip, it induces C–O cleavage through either electron transfer or vibrational excitation. The mechanisms yield products that are distinct from each other and from those of the thermal reaction[41]. Part **b** is reprinted with permission from Hla, S-W. et al. *Phys. Rev Lett.* **85**, 2777–2780 (2000). Copyright (2000) by the American Physical Society. Part **c** adapted with permission from REF.[9], American Chemical Society.

level. The original Ullmann reaction, discovered over a century ago, required super-stoichiometric Cu as a catalyst/reductant and refluxing high-boiling solvents like Me_2SO or Me_2NCHO. Tremendous efforts are still underway to find milder and greener conditions and catalysts[39]. Controlling this reaction in a STM is an innovative approach to catalysis.

Surface experiments suffer from several challenges and are typically not a viable approach to large-scale synthesis. These experiments we have discussed are all conducted under UHV and the mechanical manipulation of single atoms requires very low temperatures, which are restrictive, impractical and not scalable. Moreover, the reaction products are left bound to the substrates rather than as free molecules, and it can be difficult to determine whether the driving force of the reaction is the tunnelling current or the electric field. In the next section, more recent reactions are discussed in which these mechanistic differences are considered, and some applications of this groundbreaking approach to controlling reactivity are demonstrated.

Recent STM-driven surface reactions

The proliferation of chemical transformations controllable by a STM largely correlates with a growing interest in single-molecule electronics and device miniaturization. This interest has brought the study of charge transport behaviour in molecular junctions to the forefront of chemical and physical research. As this body of work expanded, we realized that the STM can mediate multiple reaction mechanisms. The differences between these mechanisms are often quite subtle, as can be seen with the use of the STM to locally trigger desulfurization of a tetracenothiophene on Cu(111)[9] (FIG. 1c). Two distinct reaction pathways were observed: a direct desulfurization and a two-step reaction in which the C–S bonds break sequentially. Reactivity in both pathways was induced by applying a positive bias, but the mechanisms could be controlled by altering the bias regime and the distance between the tip and the substrate. At a larger distance, only the first C–S cleavage occurred, with the second event requiring closer contact. The dominant stimulus of the first step was assumed to be the electric field, while a combination of electric field and current controlled the second event, which required a sufficiently high injection of electrons.

Another study demonstrated a STM-tip-induced S_N2-like ether cleavage of tetrahydrofuran on a Si(001) surface, which proceeded through different mechanisms, depending on the applied bias[41] (FIG. 1d). Indeed, one mechanism involves $1e^-$ transfer from the STM tip to the molecule, while the other involves inelastic

tunnelling and vibrational excitation. The products of the two reaction pathways are distinct from each other and from those of the thermal reaction. Products bound to the Si surface could be distinguished through STM imaging. These results demonstrated that typical factors that limit the S_N2 reactions, such as steric hindrance, can be overcome by using the STM on an inert surface to induce and study unconventional reaction mechanisms.

These recent examples illustrate how multiple mechanistic pathways can be operative in a STM junction. The scope of these reactions continues to broaden and more investigations into the mechanisms are required. This work also foreshadows how selectivity is as important to chemistry in a junction as it is in bulk synthetic chemistry. Either direct injection of electrons or the application of an electric field can manipulate a molecule with multiple reactive sites. By altering the bias regime such that only a single mechanistic pathway is operative, one can selectively transform a single type of moiety in a molecule.

Another important feature of a STM is that it can probe molecules on relatively inert surfaces, enabling the observation of otherwise inaccessible intermediates. For example, electrical current in a STM has been used to induce the formation of polyynes on thin layers of NaCl that decouple the molecule from the underlying substrate to reveal mechanistic insights into the reductive rearrangement of a 1,1-dibromoolefin to an alkyne[42] (FIG. 2a). Electrons from the probe tip cleave C–Br bonds individually, triggering a 1,2-shift by atomic manipulation on the surface. The geometry of the resulting vinyl radical intermediate, which persists on the inert surface, could, thus, be measured for the first time. Another STM-induced reaction on NaCl involves conjugated molecules with two terminal alkynes that undergo intramolecular Glaser-like coupling[43]. The reaction intermediates were sufficiently long-lived to allow orbital density mapping and the observation of partially dehydrogenated intermediates (FIG. 2b). In general, manipulation of molecules on an inert surface allows one to induce and study each step of a reaction individually without the need for catalytic activity or binding of the analyte to an electrode. In this way, STM manipulation is generally applicable and we envisage that structures with increasing complexity will be fabricated and studied in the future.

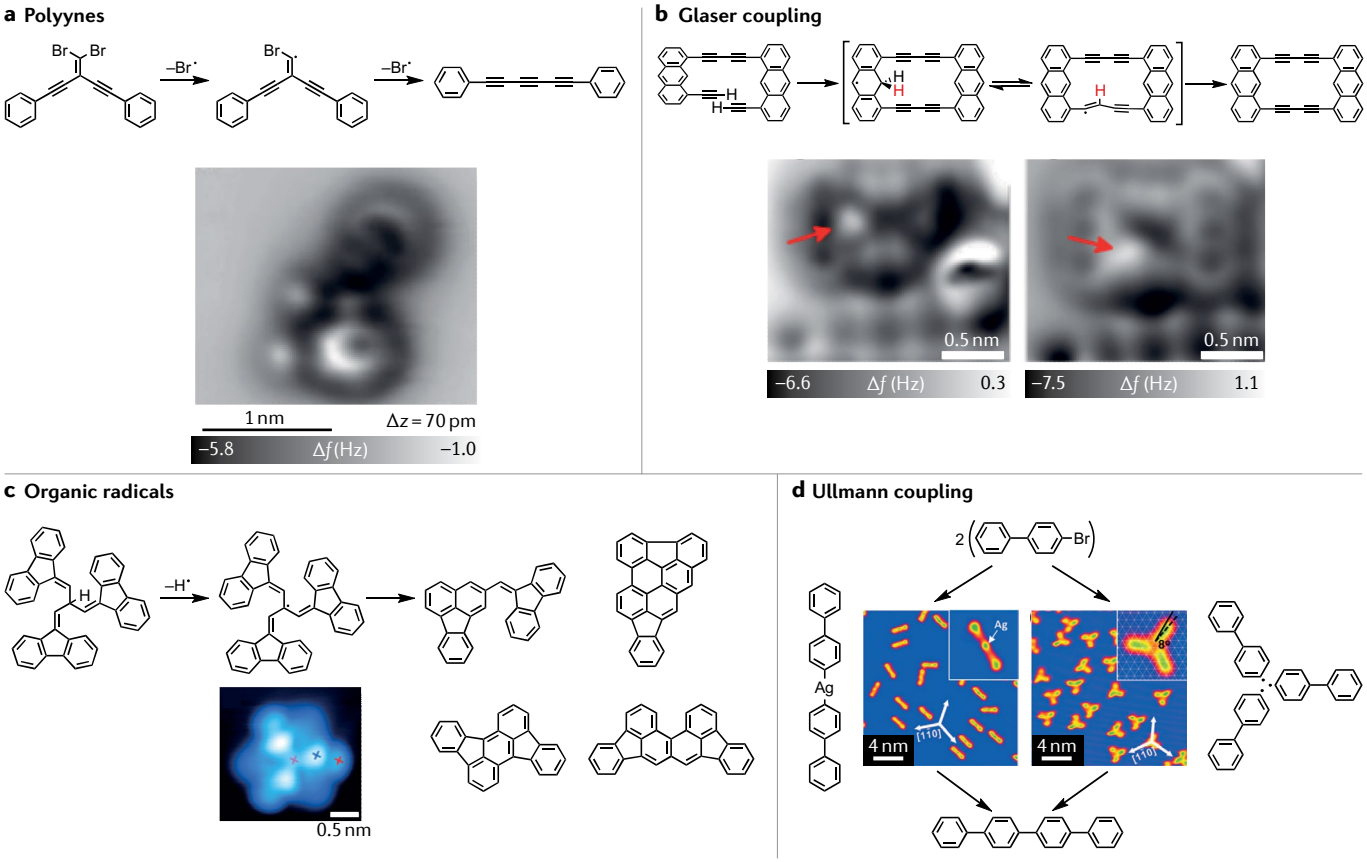

Fig. 2 | **Visualizing reaction intermediates in a scanning tunnelling microscope.** The scanning tunnelling microscope (STM) uniquely allows us to visualize reaction intermediates that are otherwise inaccessible and/or short-lived, leading to important mechanistic insights. **a** | A STM current induces the formation of a vinyl radical, an intermediate that can be visualized on the way to triyne formation[42]. **b** | Similarly, a STM tip can give observable partially dehydrogenated intermediates in intramolecular Glaser coupling[43]. **c** | Bond-resolved STM enables C(sp^3)–H cleavage and visualization of the resulting monoradical before it converts into four distinct products[48]. **d** | The STM induces Ullmann homocoupling through two pathways[50], depending on reactant concentration and areal confinement. One pathway involves surface Ag and a C–Ag–C intermediate, while the other is a metal-free radical coupling. Part **a** adapted from REF.[42], Springer Nature Limited. Part **b** adapted from REF.[43], CC by 4.0 (https://creativecommons.org/licenses/by/4.0/). Part **c** adapted with permission from REF.[48], American Chemical Society. Part **d** adapted with permission from REF.[50], Wiley.

Thermally induced surface reactions

A STM enables one to study reactions with real-space molecular imaging at the level of individual bonds. Indeed, bond-resolved STM (BRSTM) can reveal diverse species like elusive organic radical intermediates, polymers[44], polycyclic aromatic hydrocarbons (PAHs) and molecular wires. This latter class of molecules have typically proven difficult to study in a STM-BJ due to both a lack of linkers and their large size. Yet, STM has given us images of novel PAHs that have not been produced (and, perhaps, cannot be produced) by conventional organic syntheses[45]. Many of these reactions have been reviewed[46], so we, instead, detail here some recent highlights of STM capabilities that are, thus far, unachievable using the break junction technique.

Imaging reaction intermediates with BRSTM. BRSTM relies on a STM tip being functionalized with a molecule to enable resolution of the internal connectivity of individual analyte molecules — even elusive intermediates. For example, it enabled surface-catalysed cyclodehydrogenation and C–N bond formation in an extended PAH (REF.[47]). Chair-like conformations of reaction intermediates can be seen adsorbed on metal substrates. BRSTM has also been used to observe organic radicals, which form, for example, from C(sp^3)–H activation on Au(111)[48] (FIG. 2c). Studying organic radicals can afford fundamental mechanistic information, as well as give materials for molecular spintronics[49]. Isolating and structurally characterizing many of these radicals by conventional means outside a STM would present tremendous challenges because the species have short lifetimes under ambient conditions.

Ullmann coupling. Surface-assisted dehalogenative coupling is a stalwart in surface chemistry. Thermally induced Ullmann coupling on Au, Cu or Ag is a popular approach to making 2D materials. Precise control over the reaction dynamics is crucial to preparing complex molecular architectures and relies on a detailed understanding of the Ullmann coupling mechanism. The mechanism and selectivity of these reactions are sensitive to subtle changes in reactant structures, surface topology and conditions.

A recent STM study of 4-bromobiphenyl homocoupling on various surfaces showed that two mechanistic pathways exist, both leading to the quaterphenyl product. One pathway involves the linear Ag(biphenyl-4-yl)$_2$ organometallic intermediate, while the other involves three radicals interacting in a symmetric, 'clover-like' intermediate[50] (FIG. 2d). The desired pathway can be chosen by surface molecular assembly analogous to the cage effect in solution chemistry. By manipulating the concentration of reactants and confining the reaction area, one can control reaction dynamics. Further experiments revealed 'four-leaf-clover-like' formations, depending on the metal surface used, which also gave the same quaterphenyl. Overall, it would have been impossible to predict (let alone visualize) multiple parallel intermediates if one had only observed that a single product formed.

From surfaces to solutions

The reactions discussed in the preceding sections exemplify how to characterize intermediates and products using STM-specific functionalities not available with the STM-BJ method. STM imaging can distinguish between products that differ in the way they bind a surface, thereby, providing a level of detail that may be lost using a STM-BJ. Indeed, various products might each bind a surface differently and have different excitation mechanisms, yet, yield similar conductance traces when in a STM-BJ. The break junction technique is also not suitable for investigations relying on inert surfaces — electrically conductive, non-inert surfaces are required for electrodes. These materials often prevent intermediates from lingering on surfaces or may catalyse a reaction. The STM, however, can image species atop a thin layer of inert material, which, in turn, lies on a conductive surface. As the molecule–electrode connection is not a prerequisite, STM can be used to study a broader scope of mechanisms and intermediates. Indeed, molecules suitable for STM do not need functionalities for immobilization, can be poor electrical conductors and can be large or bulky.

Although the work in this section showcases the unique ability of a STM to catalyse reactions on the atomic level and provide images of intermediates and products, even recent examples present a slew of challenges that limit its synthetic utility. Single-molecule surface chemistry still requires stringent conditions and the fact that products are surface-bound detracts from the practicality relative to solution syntheses. The following sections focus on recent work that has begun to bridge the gap between these seminal experiments and the use of the technique for practical syntheses. These works establish the break junction as an important tool to probe reactivity and mechanisms of single molecules in solution, affording information that is fundamentally relevant to practical synthetic chemistry.

Nanoscale electrode-driven reactions

Myriad chemical stimuli can be exerted to induce reactivity within a STM. The electrodes can be considered chemical reagents by providing a current, an electric field, a mechanical force or by acting as an electrochemical redox agent (FIG. 3).

A redox-active molecule in an electrochemically gated junction can gain or lose 1e^-. Redox reactions require a polar solvent and a supporting electrolyte, which forms a dense double layer of ions around the nanostructured STM tip. The small exposed area of the tip and high voltage provide a strongly asymmetric field distribution that allows reactions directly at the tip. Reactions can also be activated by a current-driven excitation of vibrational modes that can cause bond rupture.

The electrode environment can also induce an electric field of variable magnitude and orientation within chemical species. This can stabilize charge-separated transition states, reaction intermediates and distribute charge to favour otherwise minor resonance structures. The lower energy barrier to these otherwise less available and less stable resonance structures and conformations

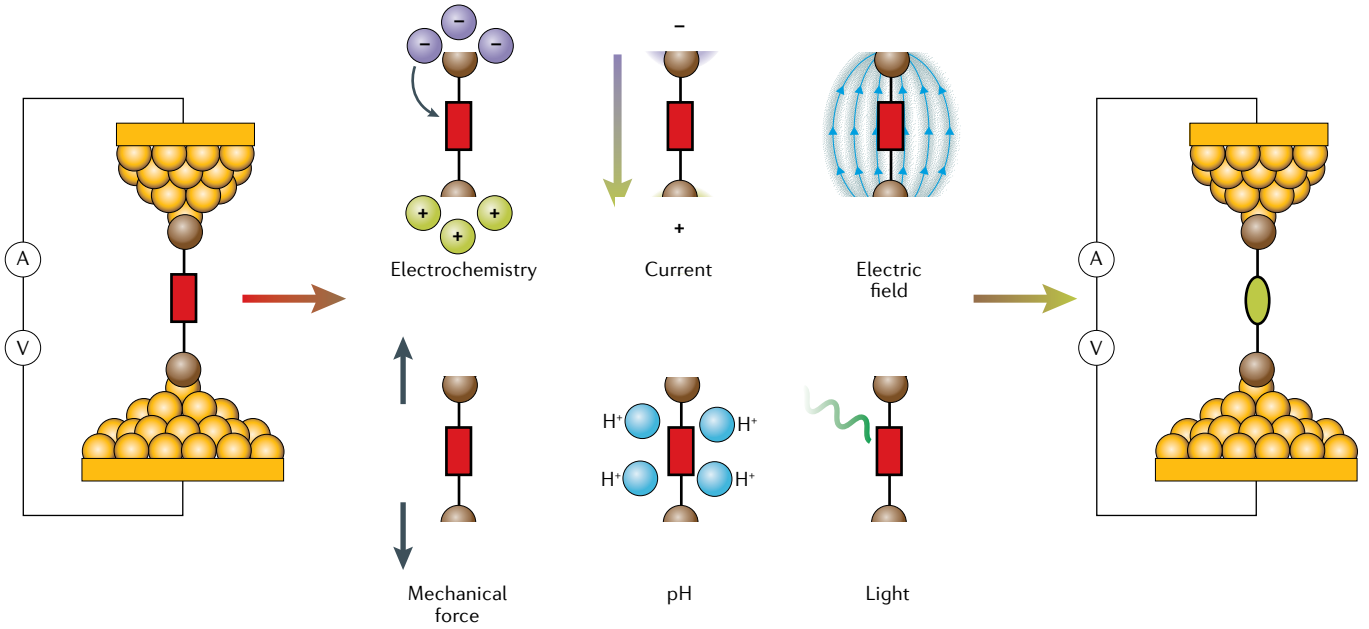

Fig. 3 | **Triggering reactions in junctions.** An applied stimulus induces a chemical transformation of a reactant (red rectangle) and directly triggers the formation or cleavage of bonds to give an immobilized product (green oval).

provides an accessible reaction pathway. Additionally, the electrodes can mechanically trigger reactions by repeatedly forming and breaking contacts between the tip and the substrate. Molecules caught in the junction can be stretched until a single bond is broken by mechanical force. This solution-based application of mechanical force is distinct from the mechanical manipulations of earlier STM-controlled reactions, in which individual atoms are relocated on a surface (FIG. 1).

Because these junction-based reactions occur in solution, one can apply other catalytic stimuli, such as acid–base catalysis or photocatalysis (FIG. 3). Thus, forming a different protonation state of a molecular backbone may induce reversible ring closure or isomerization, while protonating/deprotonating a linker may alter the coupling of the analyte molecule to the electrode. Irradiation can also excite electrons in photochromic molecules in the junction, so long as the molecules are electronically decoupled from electrodes, such that they are not quenched. Moreover, these external stimuli can be combined to create finely tuned, dual-control systems.

In situ Au contacts

When constructing organic single-molecule junctions, charge transport across the metal–molecule interface[51] is dictated by the coupling of the linker's discrete molecular orbitals to the electronic bands of the bulk metal electrodes. Therefore, analyte molecules must be thoughtfully designed and include a moiety that links it to the surface with strong electronic coupling, the synthesis of which is often challenging. Yet, direct Au–C linkages are particularly attractive[52], because they are particularly good electrical conductors. Creating a robust, low-resistance contact to Au within the junction starting from more synthetically accessible molecules is an elegant alternative. Such a solution not only introduces a new level of convenience and simplicity but also yields valuable information about M–C bonds that might be applicable to organometallic chemistry.

Organostannanes. Non-covalent Au···C linkages have been realized using C_{60}, C_6H_6 and π-stacked C_6H_6 (REFS[53–56]), but these linkage are not as robust or highly conducting as covalent Au–C bonds. This linkage has been achieved in situ using $SnMe_3$-terminated molecules that undergo transmetallation in the junction to yield direct Au–C linkages[52] (FIG. 4a). STM-BJ measurements performed on $SnMe_3$-terminated alkanes[57] revealed that, across the series of alkanes, the direct Au–C junctions showed a 100× increase in conductance compared with analogous junctions with other linkers[58–62]. The overall transmetallation was proposed to occur through a mechanism similar to a reductive elimination[63]. In any case, this study demonstrated a reproducible method for in situ formation of highly conducting metal–organic contacts. A follow-up study[64] demonstrated that slightly altering the molecular design and placing the $SnMe_3$ at the benzylic position enhanced the coupling of the electrode into the π system of the conjugated molecule, leading to an even higher conductance.

Diazonium salts. The cathodic reduction of aryldiazonium salts can also be used to form single-molecule junctions with strong covalent Au–C bonds[65] (FIG. 4b). These Au–C bonds are exceptionally stable over a long junction distance. In one study, molecular films terminated with diazonium salts at both ends underwent $1e^-$ reduction at each end, followed by release of N_2, to form covalent Au–molecule–Si junctions between Au metal and the semiconductor Si (REF.[66]). The electron-poor bis(diazonium) loses two molecules of N_2 and spontaneously attaches to both electrodes. These junctions show

a comparatively long junction lifetime of ~1 s, attributed to the robustness of the covalent Si–C and Au–C linkages[67].

Aryl iodides. Perhaps the most practical and economical approach to making in situ Au–C contacts is the use of aryl iodides[68], which are common functional groups in organic chemistry. STM-BJ measurements performed on a series of asymmetric aryl iodides elucidated the binding modes (FIG. 4c) of iodides to Au, demonstrating that both dative Au ← I and covalent Au–C linkages were formed. Covalent linkages were formed from I–C bond dissociation, the extent of which was mediated by the bias in an electrochemical environment.

Carbenes. A less ubiquitous but no less versatile class of functional groups that readily link to metals are carbenes — neutral molecules comprising a divalent C atom with a six-electron valence shell[69]. Carbene anchors have been used to form trifunctional primed contacts that create a reactive site for the in situ growth of molecular wires[70]. The M–C π bond is not only an efficient conduit for charge carriers but is also active in olefin metathesis, and was further developed for catalytic polymer growth on functionalized Ru nanoparticles[71]. This work laid the foundation for forming stable monolayers between carbenes and metals using solution-phase chemistry. Carbenes can also be implemented as highly coupled linkers in single-molecule devices. The rich chemistry and strong σ-donating ability of N-heterocyclic carbenes (NHCs) offer unique prospects for applications in nanoelectronics, sensing and electrochemistry[72–77]. Notably, however, direct linkage to Au could not be achieved with free NHCs in solution or when using vapour phase NHC-CO_2 (REFS[78,79]). Therefore, to study electron transport across single NHC-bound molecules with the STM-BJ method[80], air-stable NHC-metal chloride (NHC–M–Cl) complexes[81] with M = Au, Ag or Cu were synthesized. These NHC complexes were electrochemically reduced in situ[82,83] to form NHC–M–electrode contacts under ambient conditions (FIG. 4d). We note that this in situ electrochemical approach yielded not Au–C bonds but Au–M–C bonds (FIG. 4d), which would normally be very synthetically challenging. By performing this chemistry in situ, the conductance properties through multiple metal contact points can be studied using only one set of electrodes.

The examples above show how simple chemical reactions in the junction have enabled great progress towards enhancing the conductance of single-molecule devices. Not all of these methods are suitable for scalable processes, as many require toxic and synthetically challenging molecules and present practical challenges. Nonetheless, these advancements as a whole represent a powerful new approach to Au–C bond formation, and moving towards ubiquitous functional groups like iodides demonstrates the growing promise of these systems. Furthermore, the oxidative addition and reductive elimination steps involved in these reactions are fundamental steps in organometallic catalysis and may be implemented in other junction reactions beyond the formation of Au–C contacts. For example, the potential-dependent I–C cleavage suggests an oxidative addition at the Au surface, as was demonstrated by experiments with aryl iodides in a polar solvent that yielded Au–C bonds (FIG. 4e). This work further opened the door to manipulating chemical transformations using the electric field generated in a molecular junction. In general, the STM-BJ will undoubtedly uncover further methods of integrating common chemicals into robust circuits.

Electrochemically gated reactions

Controlling the switching between charge-transport states of a molecule in a metal–molecule junction remains one of the most challenging aspects of molecular electronics[84]. Electrochemical gating using a STM-BJ

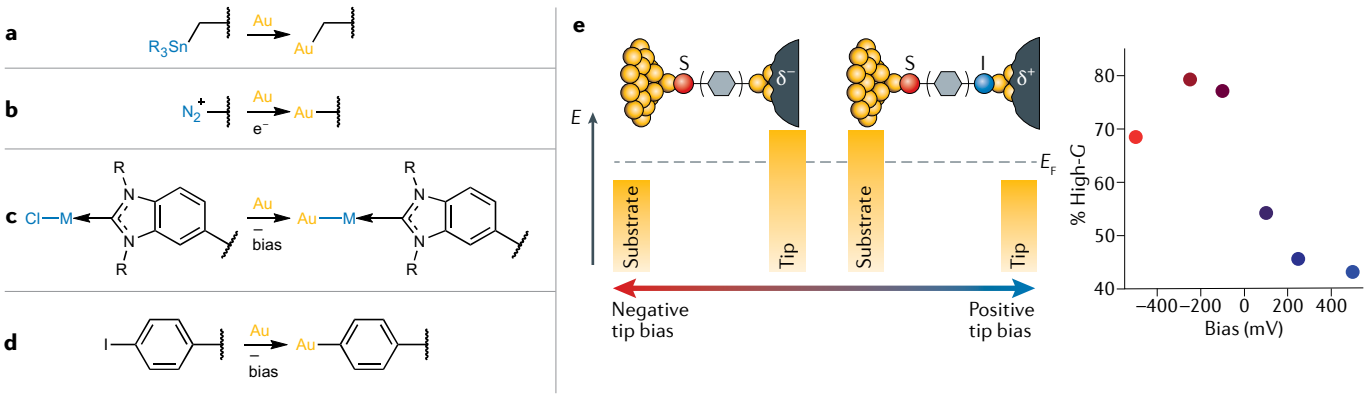

Fig. 4 | **In situ formation of covalent Au contacts using different leaving groups.** Molecules with labile groups that can be easily cleaved in the junction provide a convenient strategy to form covalent Au–C and Au–M bonds. **a** | $SnMe_3$-terminated molecules are cleaved in the junction to yield direct Au–C linkages[52,57] with a 100× increase in conductance compared with analogous oligophenylenes with two NH_2 instead of CH_2 termini. Only one terminus of the 1,4-xylenediyl linker is shown here. **b** | Aryldiazonium salts undergo in situ electrochemical reduction to form single-molecule junctions with strong covalent Au–C contacts that are stable over a long junction distance[65,66]. **c** | Aryl iodides in the scanning tunnelling microscope break junction enable both dative Au ← I and covalent Au–C linkages. **d** | Air-stable ClM(N-heterocyclic carbene) complexes undergo electrochemical reduction to form Au–M–C bonds under ambient junction conditions[80]. **e** | Aryl iodides exhibit a bias-dependent oxidative addition process at the junction. With a Au ← (Me)S(1,4-$C_6H_4)_n$I → Au (n = 1–4) dative precursor, oxidative addition to Au is promoted at more negative bias, as is evident from the increase in the fraction of junctions in the high conductance (high-G) state, which corresponds to Au ← (Me)S(1,4-$C_6H_4)_n$–Au and features a C–Au bond. The low-conductance precursor prevails at high bias values. Part **e** adapted with permission from REF.[68], American Chemical Society.

(FIG. 5a) is an attractive method to control and study bias-induced conductance switching, and it also presents an appealing way to discover and study nanoscale electrochemical catalysis. It obviates the need for exogenous chemicals or stimuli to induce reversible bond breakage and formation in molecular junctions. Indeed, using only the potential difference between the electrodes or the current through the molecule, one can alter the conductivity with large conductance ratios G_{on}/G_{off}. This section describes some of the notable electrochemical gate-driven STM-BJ switches and the chemical reactions that drive the switching behaviour.

Redox switches. Redox-active molecules are perfect candidates for reversible junction reactions. Anthraquinones (AQs) are particularly attractive systems to study switchable electrical properties, lending insight into redox and quantum interference behaviour[85]. The reversible conductance tuning of two isomeric AQ derivatives (FIG. 5b) was demonstrated using electrochemical-gating-induced switching[84]. A reductive potential reversibly reduced 1,4-disubstituted or 1,5-disubstituted anthroquinones to the corresponding hydroquinones, which are returned back to AQs on being subjected to an oxidative bias. The hydroquinones are much better conductors, and, in the case of 1,5-disubstitution, the conductance changes by more than one order of magnitude. Notably, the change in the redox state of these molecules involves both breakage and formation of new O–H bonds. This process is highly reversible, as evidenced by the G_{on}/G_{off} ratio being stable over three consecutive cycles.

A potential can also be applied in tandem with pH changes to induce switching, which has been demonstrated in junctions comprising 1,2-bis(4-pyridyl) ethylene between Ni electrodes[86] (FIG. 5c). Two distinct conductance states were observed on varying pH, and the pH value at which switching was observed could be varied by adjusting the electrochemical gate potential. The mechanism involves protonation/deprotonation of a pyridine N atom and is observable in a single measurement, suggesting that the switching is stochastic and chemically (as opposed to structurally) driven. This simultaneous control of pH and gate potential highlights how a STM-BJ can be used to study acid–base equilibria of single molecules, including the observation of discrete H^+ transfers to and from a single molecule immobilized in a metal–molecule–metal junction. In principle, this sensor could be used to measure local pH. These studies demonstrate how the STM-BJ allows facile, controlled switching of a single redox-active molecule. Detecting such processes at the single-molecule level provides insight into controlled transformations that are typically inaccessible through conventional bulk synthetic techniques[87,88].

Externally modulated switches. In addition to chemical reactions in a STM-BJ induced by junction-based mechanisms, reactions can also be controlled in the junction

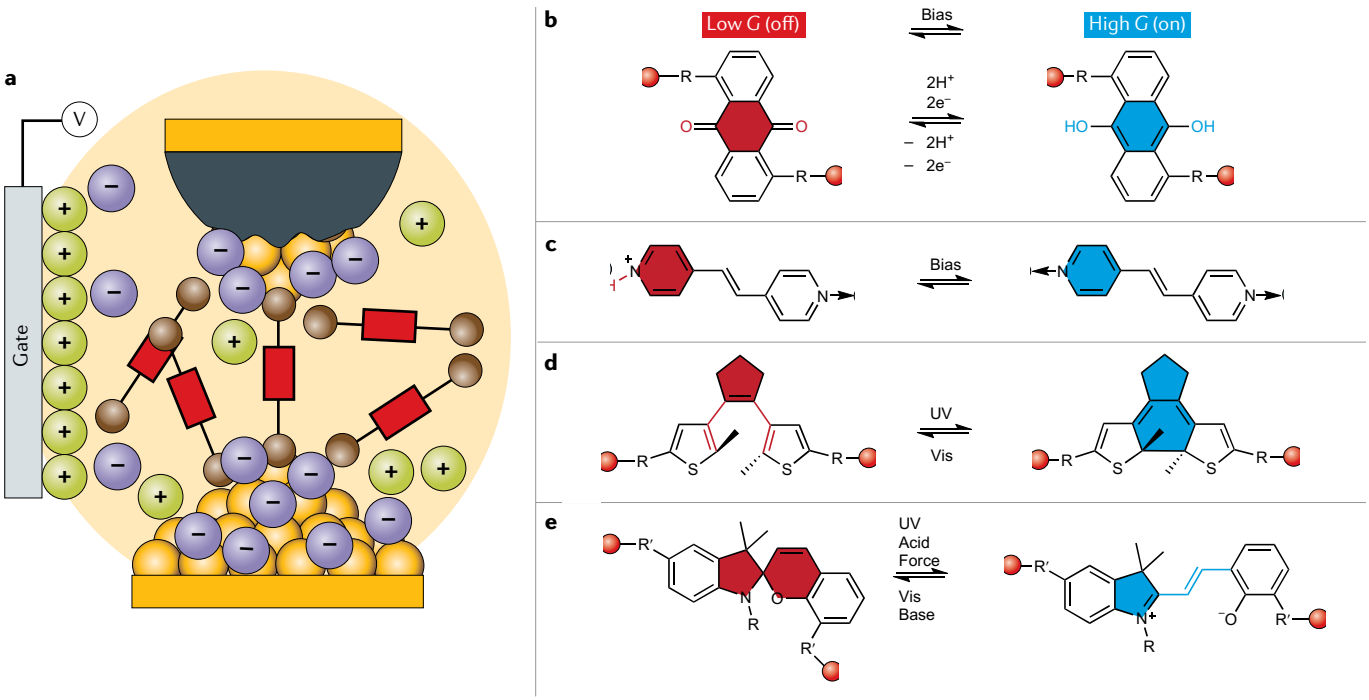

Fig. 5 | **Electrochemically gated switches in a scanning tunnelling microscope break junction. a** | Schematic of a three-electrode electrochemically gated junction. The bias between the two working electrodes and the gate voltage can be controlled simultaneously. The tip is coated with a chemically inert wax such that the area of Au exposed to solution is drastically lowered compared with the substrate. A dense double layer of ions promotes electrochemical transformations. **b** | 1,5-Disubstituted anthroquinones undergo reversible electrochemically gated reduction to the corresponding hydroquinones, which are much better electrical conductors[84]. **c** | An applied potential is used in tandem with pH changes to induce switching in junctions where 1,2-bis(4-pyridyl)ethylene spans two Ni electrodes[86]. **d** | Photochromic dithienylcyclopentenes undergo optoelectronic switching on irradiation, which causes a change of the π-conjugation and conductance of the molecule[89,90]. **e** | Spiropyrans respond to numerous orthogonal stimuli, including light, pH and mechanical force, to switch between open and closed forms[120]. UV, ultraviolet; Vis, visible.

using external stimuli. These stimuli replace exogenous chemicals or catalysts that are used in prototypical synthetic reactions. The reactions discussed in this section involve two of the more commonly applied stimuli — light[89–97] and mechanical force[98,99] — but are, by no means, an exhaustive list, as many other modes of catalysis can be incorporated (FIG. 3). External stimuli compatible with the junction range from light, mechanical force, pH (REF.[100]), voltage[101–108], stereoelectronic effects[109] and electric[110–112] or magnetic fields[113–115]. Although these reactions are not strictly controlled by the junction, they are frequently incorporated into on ↔ off switches that are essential to nanoelectronics. Many of the observations regarding fundamental processes made at the single-molecule level cannot be gleaned from bulk chemistry and inform our broader understanding of these chemical processes.

Optical switches have garnered widespread interest for their applications in molecular electronics[116] and many other emerging fields, such as biomimetic catalysis[117] and photopharmacology[118]. Photochromic dithienylcyclopentenes have been used to achieve optoelectronic switching[89] both in and out of the junction (FIG. 5d). Outside of the junction, on irradiation, the covalent C–C bonds in the switchable moiety can be selectively broken or formed, depending on the wavelength of light used, resulting in a change of the conjugation and conductance of the molecule. In the junction, however, only an irreversible on → off switch is possible because Au electrodes quench the first excited state of the open (off) form, preventing the reversal back to the closed (on) form. The quenching of a molecule by metal electrodes presents a general challenge to translating bulk chemistry to single-molecule studies. Quenching can be avoided by electronically decoupling the active site of a molecule from the electrodes, with diarylethylenes now being a common moiety in molecular switches. A modified diarylethylene covalently linked between graphene electrodes is a reversible photoswitch at room temperature[90]. The altered structure of the molecule decreases coupling with the electrode to prevent problematic quenching. The high ratio of drain currents I_{on}/I_{off} >100 was stable over 100 cycles. This adjustment highlights the importance of chemical design and the structure–function relationship between molecules, enhancing their utility in electronics, as well as for adapting bulk chemistry to the single-molecule junction.

Switches in the junction can also be manipulated with orthogonal external stimuli to form logic gates[119] by selectively stimulating a pH-sensitive moiety and a photochromic moiety to obtain four possible conductance states. Additionally, stimuli-specific spiropyran devices[120] have been fabricated to use mechanical and chemical stimuli to probe bond strength. In general, spiropyran is a particularly prominent moiety due to the stark contrast in properties with its isomeric merocyanine form (FIG. 5e). Interconversion between these forms can be harnessed in a single-molecule device for switching applications. These studies demonstrate the utility of a STM-BJ to investigate reactions at the single-molecule level by breaking and reforming junctions. They highlight the ease with which a STM-BJ can monitor reactivity but also reveal challenges that arise with in situ reactions that do not occur in the bulk, such as quenching of molecules by electrodes. Indeed, the behaviour of the molecule in bulk solution will differ to its behaviour in a STM-BJ in this regard, and it is important to identify and address these challenges to develop the field of research.

Electrostatic reactions

One of the most promising and practical aspects of break junction chemistry is the ability to catalyse reactions using an electric field. Catalysing reactions involving redox-inactive molecules in an electric field has long been theorized[121] but only recently been realized[121–127]. Solution-based electric field catalysis offers an economical, environmentally friendly and synthetically straightforward alternative to conventional methods that use exogenous chemical catalysts. Electric fields facilitate reactions of non-redox-active molecules by stabilizing transition states or minor charge-separated resonance contributors[88,128–130]. Access to these otherwise less accessible forms can potentially alter or tune selectivity outcomes[124,130–133] and, depending on the alignment of these forms in the field, can manipulate the kinetics and thermodynamics of non-redox processes. As such, electric field catalysis is potentially applicable to a wide scope of reactions, yet, it remains incompletely understood[127,134] and underdeveloped.

Two major challenges in electric field catalysis are: (i) precisely orienting the direction of the electric field with the reaction coordinate of a molecule and (ii) applying such a highly oriented and intense field. A STM-BJ set-up offers a viable route to realizing this because the solution around the nanoelectrodes is continuously exposed to a high electric field (FIG. 6a).

Over time, all molecules in a solution can be exposed to an applied electric field through diffusion and local turbulence from the moving tip. In the following sections, we focus on three examples of how an electric field catalyses an isomerization, bimolecular reaction and an intramolecular aromatization of non-redox-active molecules.

Bimolecular reactions. The Diels–Alder reaction between thiolate-anchored furan and norbornene dienophile derivatives was the first bond-forming process between two non-redox-active species to be accelerated by an external electric field[88] (FIG. 6b). The preassembled layer of dienophile on the substrate allowed for unambiguous orientation of the double bond, whereas the tip-tethered diene was free to rotate and approach the dienophile in any of four possible orientations. The preassembled substrate layer was aligned with the electric field such that formation of only one low-energy product was sensitive to the field. A fivefold increase in the frequency of the reaction was observed when a large negative bias was applied across the junction, suggesting that the field facilitates electron flow from dienophile to diene, stabilizing an otherwise minor resonance contributor.

Although this Diels–Alder reaction was conducted on a preassembled surface, it could not be replicated in

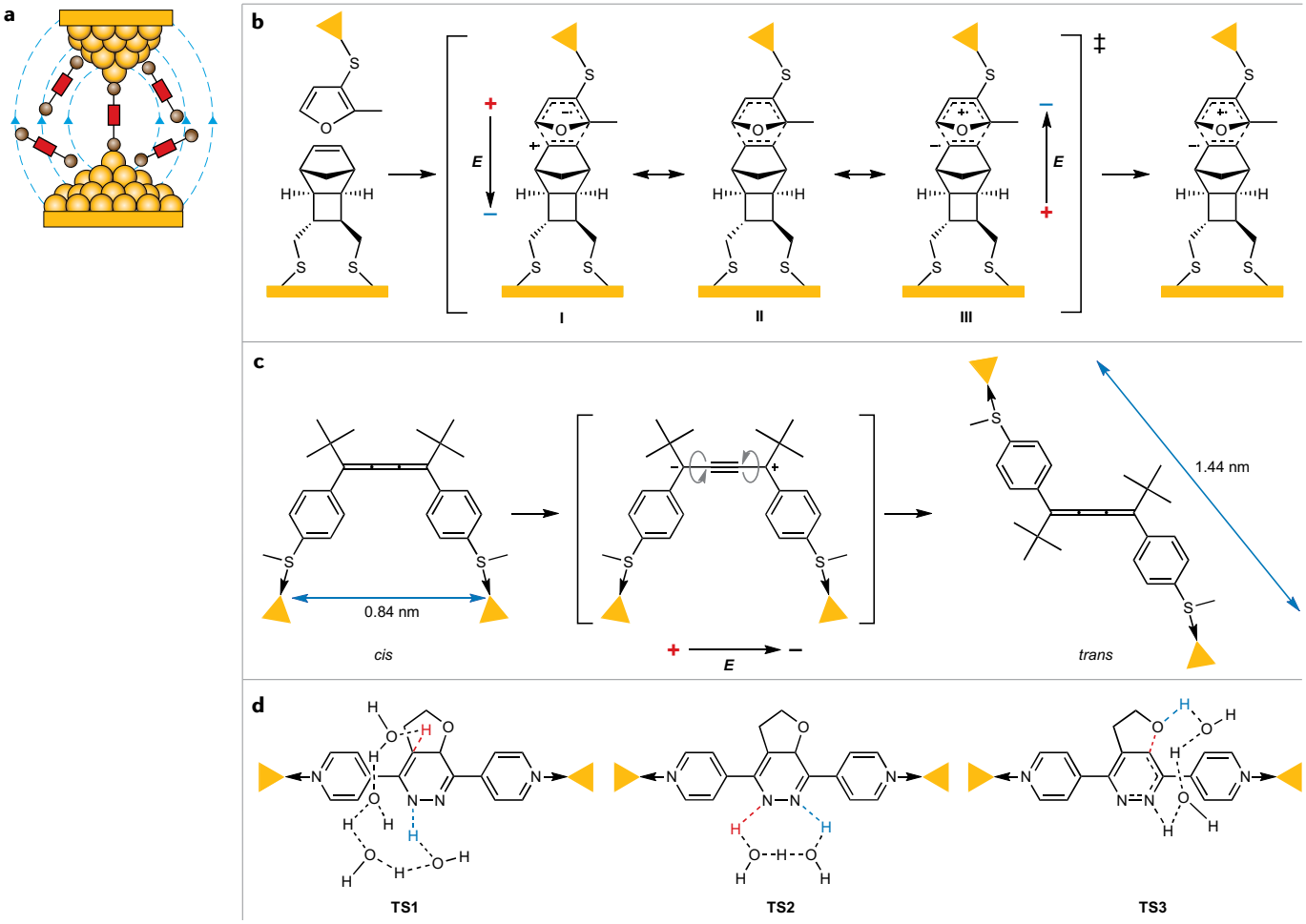

Fig. 6 | **Electric-field-driven reactions in a scanning tunnelling microscope. a** | The electric field between a scanning tunnelling microscope tip and substrate is also present across the single-molecule junction. **b** | A bimolecular, non-redox bond-forming process accelerated by an external electric field was demonstrated in the case of the Diels–Alder reaction of a tip-tethered furan and a surface-anchored norbornene derivative[88]. The scanning tunnelling microscope break junction supplied the electric field and the reaction was monitored according to changes in conductance and molecular plateau lengths that are characteristic of the reactants and products. The electric field between the tip and substrate facilitates electron flow from dienophile to diene, stabilizing an otherwise minor resonance contributor. **c** | Cumulenes undergo *cis–trans* isomerization in the presence of an electric field with an increased conversion rate compared with thermally triggered solutions[136]. The reaction occurs throughout the solution near the junction. The dramatic difference in the inter-electrode distance allows for the reaction to be monitored. The electric field stabilizes a non-canonical zwitterionic resonance structure to facilitate the isomerization. **d** | A cascade involving an inverse-electron-demand Diels–Alder reaction and subsequent aromatization is catalysed in the junction by an electric field[137]. The field aligns only with the aromatization process and stabilizes the key transition states (TSs) in the second step.

solution and suffered from an ultra-low conversion rate of a few molecules per hour. Furthermore, the results were never verified by comparison with products formed ex situ. This work, however, importantly demonstrated that the scope of electric field catalysis includes non-redox processes, vastly expanding the applicability of electrostatically catalysed reactions[135].

Isomerization. Recently, the local electric field in the STM-BJ was used to catalyse the *cis–trans* isomerization of cumulenes[136] (FIG. 6c). The external electric field increased the rate of isomerization and changed the distribution of *cis* and *trans* products. The conductance signatures of the *trans* and *cis* isomers are distinct because the isomerization leads to a large change in displacement of the electrodes (FIG. 6c), making it easy to monitor the reaction. The method is quantitative and, at a positive bias, a solution of *cis* cumulene in the STM-BJ was converted to predominantly *trans*. Furthermore, by increasing the reaction time, enough *trans* product can be generated for the sample to be analysed by high-performance liquid chromatography. The number of molecules converted far exceeds the number of single-molecule junctions formed, indicating that the reaction is catalysed by the electric field and occurs throughout the solution near the tip.

The mechanistic rationale for this reaction illustrates the simple yet elegant way that an electric field can alter the selectivity and feasibility of a non-redox process. Density functional theory calculations concerning how the electrostatic field might alter reaction kinetics and thermodynamics to favour the *trans* isomer indicate that the

electric field lowers the rotational barrier to isomerization. Thus, the electric field stabilized the otherwise less prominent polar zwitterionic resonance structure (FIG. 6c), which can undergo relatively free rotation around its terminal C–C bonds. This work demonstrates how solution-based, electric-field-driven isomerization in a non-polar solvent can change the product distribution, opening the door for more electrostatically controlled solution chemistry.

Aromatization. Tuning the orientation between an external electric field and a reaction axis can selectively catalyse an individual step of a cascade reaction. For example, a cascade involving an inverse-electron-demand Diels–Alder reaction before an aromatization forms a fully conjugated, electrically conducting final product[137] (FIG. 6d). Using a mechanically controlled break junction in the presence of an electric field, only the second step of the two-step cascade is accelerated. The reaction axis of the Diels–Alder step is orthogonal to that of the field, but the aromatization is aligned. Thus, the field accelerates the aromatization step by an order of magnitude with applied bias but the rate of cyclization remains unaffected. The ability to accelerate selected steps in a multistep process could be used to manipulate or even toggle between a kinetically or thermodynamically favoured distribution of products in a multistep process.

The future of electric field catalysis. As a whole, the reactions we have described highlight scalable applications of solution-based electric field catalysis and the possible synthetic applications of chemistry discovered in the break junction. Reactions proceed under ambient conditions and the local electrical potential that drives them obviates the need for exogenous chemicals. These reactions are the closest facsimile to practical bulk chemistry because they occur in the solution around the tip and do not require junction formation. Thus, the scope of these reactions can encompass substrates without aurophilic groups such as thiolates or thioethers that are usually necessary to bind an Au surface[136]. Simultaneously, the reactions also benefit from the ability to study them one molecule at a time, as the break junction allows us to monitor reaction kinetics.

Developing electric field catalysis as a practical synthetic tool still faces many challenges. Multiple experiments are required to glean mechanistic information and often need to be supplemented by non-junction experiments. The technique also needs to be validated by ex situ analysis of the product(s) formed. Because the distance between electrodes changes during the STM-BJ measurements, the magnitude of the field cannot be precisely determined and a quantitative measurement of field dependence is unavailable. These hurdles may be overcome by controlling nanoenvironments surrounding reaction centres, using microfluidic techniques and designing devices that allow for the application of an electric field in a confined nanoenvironment. These fundamental experiments, however, have cemented the STM-BJ as a crucially important tool to explore the burgeoning field of electrostatic catalysis.

Probing single-molecule reactions

The advents of both STM and atomic force microscopy (AFM)[138] enabled atomic-scale imaging of reactants and products, and opened the door to both monitoring and controlling reactions at the single-molecule level. Capitalizing on foundational work, more recent studies have applied these techniques to controlling chemistry in more complex systems. For example, coordination of ligands to metal atoms has been expanded beyond simple M–CO bond formation to encompass larger, more intricate organic molecules[11,139]. Tip-induced radical formation and dehalogenation have induced intramolecular rearrangements and ring formation in polycyclic aromatic systems[140,141]. Importantly, these tip-induced reactions are in contrast with the thermal single-molecule surface reactions that are achieved through annealing. STM-AFM has been used to resolve thermally assisted reactions, such as complex cyclization cascades[142] and many rearrangements and couplings[45,46]. Much of this work has been reviewed previously[143]. In this section, we highlight some of the most recent achievements in single-molecule reactions and discuss the evolution of the field to include new techniques, like the break junction, that allow us to control not only surface reactions at the single-molecule level but solution chemistry as well.

Low-temperature STM-AFM has been used to synthesize the highly elusive carbon allotrope cyclo[18]carbon on Cu(111)[144]. Starting with $C_{24}O_6$, voltage pulses were applied for a few seconds at a time, resulting in the extrusion of two, four or six CO moieties and a 13% yield of the fully decarbonylated product C_{18} (FIG. 7a). This molecule could be deliberately reversibly switched between neutral and anionic states, resulting in different geometries imaged by STM and AFM. Furthermore, by applying an elevated bias, two partially decarbonylated molecules could be covalently fused. This work is a milestone in the applicability of tip-induced chemistry to achieve elusive reactivity and capture molecules that cannot be studied using more conventional synthetic techniques, though the constraints of on-surface reactions still apply. The reaction requires an inert surface and low temperature (5 K), and sublimation of the material onto Cu(111) induced partial decarbonylation and dissociation of CO molecules prior to tip modulation.

One of the unique aspects of the break junction technique is the ability to effect and observe reactions in a solution that occur one molecule at a time[6,7,142]. Several older approaches to monitor single-molecule reactivity require preassembled molecules on a surface. Thus, we stress here the first observations of controlled bond formation between two molecules dispersed in solution. These solution-based proof-of-principle reactions much more closely resemble conventional reactions, which will ultimately prove crucial for gaining insight into real-world applications and phenomena. Overall, we have a new methodology to interrogate chemical reactions at the single-molecule level and to precisely make molecular nanostructures that are otherwise challenging to prepare by conventional bulk methods.

The first demonstration of a truly single-molecule bond formation process in solution was the electrochemical manipulation of a Au ← N contact to modify

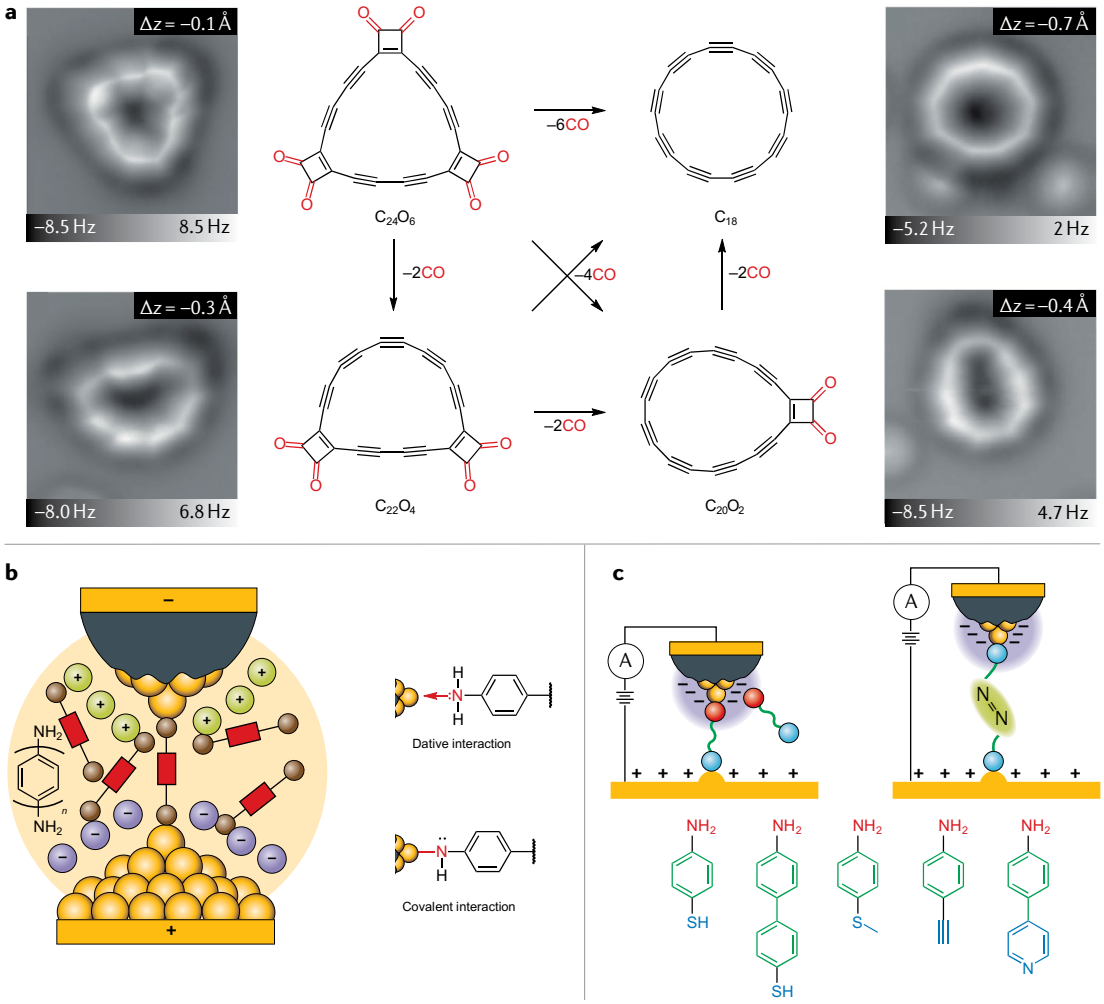

Fig. 7 | **Inducing reactivity one molecule at a time. a** | Voltage pulses dissociated a hexacarbonyl precursor to afford the carbon allotrope cyclo[18]carbon (C_{18}) on Cu(111) surface[144]. Atomic force microscopy images show the molecule sequentially losing pairs of CO groups. **b** | Oligophenylenediamines can bind a junction through distinct modes. The electrochemical manipulation of the Au ← N contact modifies the charge transport across the interface, resulting in oligophenylenediamine wires with low, high and ultra-high conductance states[145]. The difference in conductance is attributed to the increasingly covalent nature of the Au ← N bond under an oxidative bias. **c** | Two aniline molecules can undergo oxidative homocoupling at an applied scanning tunnelling microscope break junction bias to make azobenzenes[154]. Part **a** adapted with permission from REF.[144], AAAS. Part **c** adapted with permission from REF.[154], Wiley.

charge transport across the interface[145] (FIG. 7b). Using a series of oligophenylenediamine wires, the authors demonstrated that an oxidizing bias led to in situ formation of a new type of Au–N bond in the break junction. Normally, amines bind selectively to undercoordinated Au atoms through dative interactions[146,147], but by changing the magnitude of the positive bias in the STM-BJ, the anilines existed in three distinct conducting states. The higher conductance states represented newly formed covalent bonds between the Au and N, analogous to the self-assembly of thiolate monolayers on a Au surface[148–151]. The ultra-high conductance state delivered the highest reported conductance values for all known oligophenylene contacts[56,152,153], achieving better electronic coupling in situ than covalent Au–S or Au–C bonds[153].

A subsequent study showed that a series of asymmetric anilines could undergo in situ electrooxidative homocoupling in the STM-BJ to form azobenzenes[154] (FIG. 7c). Oxidative coupling reactions are important for chemical synthesis and bioconjugation[155], and are alternatives to traditional cross-coupling strategies[156]. Developing nanocatalysts and electrosynthetic techniques to effect such transformations offers a versatile and environmentally friendly synthetic alternative[157–159]. In the STM-BJ, anilines undergo a 'one-pot' selective oxidative coupling to form azobenzenes on the nanostructured Au STM tip under oxidative bias. The coupling is rapid, reproducible and quite general, being amenable to a variety of anilines with different aurophilic linkers and backbone lengths (FIG. 7c). The selective synthesis of geometric isomers depending on the linker has also been demonstrated. Notably, in the case of 4-(4-pyridyl) aniline, the *cis* isomer forms instead of the energetically more stable *trans* isomer that forms in bulk synthesis. This unexpected result demonstrated how the junction

can impart new selectivity to a reaction. Furthermore, sequential coupling of complementary anilines could be achieved in the junction, resulting in complex molecular architectures that are more synthetically onerous. Thus, chemicals that were not formed ex situ could still be accessed and probed.

Together, these reactions stress the unique characteristics of reactions in the junction, which are enumerated using the in situ formation of azobenzenes as a demonstrative example. First, the voltage necessary to trigger the electrooxidation at the tip is lower than the oxidation potential of aniline and its derivatives[160,161], suggesting that the redox transformation in the junction is facilitated by the attachment of the anilines to undercoordinated Au active sites. This low voltage contrasts with homogeneous bulk syntheses requiring strong oxidants, often in stoichiometric quantities[162]. Second, the immediate formation of the longer molecule, as evidenced by a characteristic conductance signature, indicates that an individual aniline caught in the single-molecule junction undergoes $1e^-$ oxidation by the Au tip to initiate the reaction. After the observation of the longer azobenzene, if the bias is then decreased, only the shorter anilines are observed, reinforcing the concept that only the molecules caught in the junction can be transformed in this case. Overall, there is only a low percentage of longer molecules in solution and a small probability of measuring them, once the bias is decreased. This behaviour further contrasts reactions such as the isomerization of cumulenes, where the bulk of the solution species are converted.

The above solution-based, single-molecule reactions exemplify how the STM-BJ offers unprecedented and exquisitely precise control over bond formation. These reactions are performed under ambient conditions and require no exogenous chemicals or preassembled molecular layers. Observing and controlling these nanoscale processes in individual molecules promises levels of precision beyond those achieved through traditional ensemble techniques. The experimental implementation of such concepts, however, remains a major challenge. Although the single-molecule reactions are not yet practical for large-scale synthesis, the control over single-molecule bond formation may shed light on mechanisms for synthetic redox reactions and illuminate new avenues for molecular design. For instance, the STM-BJ can be used to apply a large, directional electric field across a molecule to investigate its effect on the reactivity of the system. This strategy is a relatively easy approach to testing a number of reactions, and the understanding gathered through these measurements could be used to develop new catalysts de novo with built-in electric fields in the form of charged residues. These studies and similar ongoing efforts will drive the fundamental understanding of nanoscale chemical and physical phenomena.

Conclusion and outlook

The reactions detailed in this Review have opened the door for detailed interrogations of reaction chemistry. Instruments originally built for imaging and molecular characterization have become powerful reaction tools. Manipulations of single molecules bound to metal surfaces have demonstrated exquisite control over chemical processes. Break junction techniques have expanded these capabilities to include reactions in solutions, obviating the need for stringent conditions such as UHV and low temperatures or additional steps such as chemical deposition and product extraction. Solution techniques can accommodate organometallic and organic reactions in which products freely diffuse away from the electrodes in solution. Complementary to the break junction method is the use of STM alone, which is amenable to larger molecules and intermediates, allowing reactions on inert surfaces to be studied in greater detail than ever before. These reactions span a wide range of transformations, including bimolecular reactions, as well as isomerizations and rearrangements that involve breakage and formation of new bonds.

Synthesizing and probing single molecules with the STM tip in solution offers a deep understanding of single-molecule processes and may lead to new discoveries in bulk solution chemistry. By highlighting and categorizing these achievements, one can see how close examination of the chemistry that occurs in a STM informs a variety of reaction types and modes of catalysis, including photochemistry, electrochemical and electric field catalysis, organometallic chemistry and more. Together, chemists and physicists are now presented with the challenge of developing these reactions in a practical and scalable way that is relevant to synthetic chemistry and molecular electronics. A crucial area of exploration will be the design of junctions that accommodate bulk transformations. Another important capability will be integrating the ability of a STM to monitor reactions in situ with more conventional techniques for analysing products, like nuclear magnetic resonance spectroscopy or mass spectrometry. We may then no longer need multiple experimental conditions or to supplement junction studies with the non-junction experiments that are presently required to glean mechanistic insight and validate some results. Furthermore, each niche area of catalysis will encounter its own challenges. For example, electrostatic reactions would benefit from a method to quantify the magnitude of the electric field dependence. Similarly, the performance and endurance of molecular switches that incorporate orthogonal stimuli such as photoexcitation would benefit from new methods to prevent quenching by the electrodes. Finally, reactions that occur only when molecules are held between the electrodes are the furthest from being developed for large-scale synthesis, yet offer the most precise control over reactivity. These experiments, however, could now be used as test beds for catalytic systems, providing a rapid and robust approach to probing the effect of directional electric fields on molecules and reactions.

To approach the practical hurdles before us, we first need to address the questions about the rules that govern chemistry in junctions. It is imperative that these reactions be interrogated in the same way that bulk synthetic chemistry is assessed with the familiar chemistry vernacular. What kind of selectivity can be achieved with these reactions? What energy barriers can be overcome by using the junction to catalyse reactions? Can the kinetic

and thermodynamic influences of the junction be bridled in a way that we achieve the requisite control over chemical behaviour? As junction reactions are incorporated into the canon of chemical synthesis, answers to these questions will emerge, unveiling a roadmap for future application and expansion.

Published online 25 August 2021

1. Skubi, K. L., Blum, T. R. & Yoon, T. P. Dual catalysis strategies in photochemical synthesis. *Chem. Rev.* **116**, 10035–10074 (2016).
2. Twilton, J. et al. The merger of transition metal and photocatalysis. *Nat. Rev. Chem.* **1**, 0052 (2017).
3. Wang, F. & Stahl, S. S. Merging photochemistry with electrochemistry: functional-group tolerant electrochemical amination of C(sp^3)–H bonds. *Angew. Chem. Int. Ed.* **58**, 6385–6390 (2019).
4. Zhang, W., Carpenter, K. L. & Lin, S. Electrochemistry broadens the scope of flavin photocatalysis: photoelectrocatalytic oxidation of unactivated alcohols. *Angew. Chem. Int. Ed.* **59**, 409–417 (2020).
5. Kim, H., Kim, H., Lambert, T. H. & Lin, S. Reductive electrophotocatalysis: merging electricity and light to achieve extreme reduction potentials. *J. Am. Chem. Soc.* **142**, 2087–2092 (2020).
6. Lee, H. J. & Ho, W. Single-bond formation and characterization with a scanning tunneling microscope. *Science* **286**, 1719–1723 (1999).
7. Hla, S., Bartels, L., Meyer, G. & Rieder, K. Inducing all steps of a chemical reaction with the scanning tunneling microscope tip: towards single molecule engineering. *Phys. Rev. Lett.* **85**, 2777–2780 (2000).
8. Minato, T. et al. Tunneling desorption of single hydrogen on the surface of titanium dioxide. *ACS Nano* **9**, 6837–6842 (2015).
9. Borca, B. et al. Electric-field-driven direct desulfurization. *ACS Nano* **11**, 4703–4709 (2017).
10. Ohmann, R., Vitali, L. & Kern, K. Actuated transitory metal–ligand bond as tunable electromechanical switch. *Nano Lett.* **10**, 2995–3000 (2010).
11. Mohn, F. et al. Reversible bond formation in a gold-atom–organic-molecule complex as a molecular switch. *Phys. Rev. Lett.* **105**, 266102 (2010).
12. Liljeroth, P., Repp, J. & Meyer, G. Current-induced hydrogen tautomerization and conductance switching of naphthalocyanine molecules. *Science* **317**, 1203–1206 (2007).
13. Simic-Milosevic, V., Mehlhorn, M., Rieder, K. H., Meyer, J. & Morgenstern, K. Electron induced ortho-meta isomerization of single molecules. *Phys. Rev. Lett.* **98**, 116102 (2007).
14. Maksymovych, P., Sorescu, D. C., Jordan, K. D. & Yates, J. T. Collective reactivity of molecular chains self-assembled on a surface. *Science* **322**, 1664–1667 (2008).
15. Neël, N., Lattelais, M., Bocquet, M. L. & Kröger, J. Depopulation of single-phthalocyanine molecular orbitals upon pyrrolic-hydrogen abstraction on graphene. *ACS Nano* **10**, 2010–2016 (2016).
16. Shen, T. C. et al. Atomic-scale desorption through electronic and vibrational excitation mechanisms. *Science* **268**, 1590–1592 (1995).
17. Serrate, D., Moro-Lagares, M., Piantek, M., Pascual, J. I. & Ibarra, M. R. Enhanced hydrogen dissociation by individual Co atoms supported on Ag(111). *J. Phys. Chem. C* **118**, 5827–5832 (2014).
18. Qiu, X. H., Nazin, G. V. & Ho, W. Mechanisms of reversible conformational transitions in a single molecule. *Phys. Rev. Lett.* **93**, 196806 (2004).
19. Alemani, M. et al. Electric field-induced isomerization of azobenzene by STM. *J. Am. Chem. Soc.* **128**, 14446–14447 (2006).
20. Lastapis, M. et al. Picometer-scale electronic control of molecular dynamics inside a single molecule. *Science* **308**, 1000–1003 (2005).
21. Iancu, V., Deshpande, A. & Hla, S. W. Manipulating Kondo temperature via single molecule switching. *Nano Lett.* **6**, 820–823 (2006).
22. Henningsen, N. et al. Inducing the rotation of a single phenyl ring with tunneling electrons. *J. Phys. Chem. C* **111**, 14843–14848 (2007).
23. Simic-Milosevic, V. & Morgenstern, K. Bending a bond within an individual adsorbed molecule. *J. Am. Chem. Soc.* **131**, 416–417 (2009).
24. Yongfeng, W., Kröger, J., Berndt, R. & Hofer, W. A. Pushing and pulling a Sn ion through an adsorbed phthalocyanine molecule. *J. Am. Chem. Soc.* **131**, 3639–3643 (2009).
25. Grill, L., Rieder, K. H. & Moresco, F. Exploring the interatomic forces between tip and single molecules during STM manipulation. *Nano Lett.* **6**, 2685–2689 (2006).
26. Grill, L. et al. Rolling a single molecular wheel at the atomic scale. *Nat. Nanotechnol.* **2**, 95–98 (2007).
27. Kudernac, T. et al. Electrically driven directional motion of a four-wheeled molecule on a metal surface. *Nature* **479**, 208–211 (2011).
28. Gimzewski, J. K. & Joachim, C. Nanoscale science of single molecules using local probes. *Science* **283**, 1683–1688 (1999).
29. Jung, T. A., Schlittler, R. R., Gimzewski, J. K., Tang, H. & Joachim, C. Controlled room-temperature positioning of individual molecules: molecular flexure and motion. *Science* **271**, 181–184 (1996).
30. Eigler, D. M. & Schweizer, E. K. Positioning single atoms with a scanning tunnelling microscope. *Nature* **344**, 524–526 (1990).
31. Dujardin, G., Walkup, R. E. & Avouris, P. Dissociation of individual molecules with electrons from the tip of a scanning tunneling microscope. *Science* **255**, 1232–1235 (1992).
32. Meyer, G., Bartels, L., Zöphel, S., Henze, E. & Rieder, K. H. Controlled atom by atom restructuring of a metal surface with the scanning tunneling microscope. *Phys. Rev. Lett.* **78**, 1512–1515 (1997).
33. Bartels, L., Meyer, G. & Rieder, K. H. Basic steps of lateral manipulation of single atoms and diatomic clusters with a scanning tunneling microscope tip. *Phys. Rev. Lett.* **79**, 697–700 (1997).
34. Bartels, L., Meyer, G. & Rieder, K. Dynamics of electron-induced manipulation of individual CO molecules on Cu(111). *Phys. Rev. Lett.* **80**, 2004–2007 (1998).
35. Stipe, B. C. et al. Single-molecule dissociation by tunneling electrons. *Phys. Rev. Lett.* **78**, 4410–4413 (1997).
36. Lauhon, L. J. & Ho, W. Single-molecule chemistry and vibrational spectroscopy: pyridine and benzene on Cu(001). *J. Phys. Chem. A* **104**, 2463–2467 (2000).
37. Crommie, M. F., Lutz, C. P. & Eigler, D. M. Confinement of electrons to quantum corrals on a metal surface. *Science* **262**, 218–220 (1993).
38. Ullman, F. & Bielecki, J. Ueber synthesen in der biphenylreihe. *Ber. Dtsch. Chem. Ges.* **34**, 2174–2185 (1901).
39. Mondal, S. Recent advancement of Ullmann-type coupling reactions in the formation of C–C bond. *ChemTexts* **2**, 17 (2016).
40. Cai, J. et al. Atomically precise bottom-up fabrication of graphene nanoribbons. *Nat. Lett.* **466**, 470–473 (2010).
41. Mette, G. et al. Controlling an S_N2 reaction by electronic and vibrational excitation: tip-induced ether cleavage on Si(001). *Angew. Chem. Int. Ed.* **58**, 3417–3420 (2019).
42. Pavliček, N. et al. Polyyne formation via skeletal rearrangement induced by atomic manipulation. *Nat. Chem.* **10**, 853–858 (2018).
43. Albrecht, F. et al. Intramolecular coupling of terminal alkynes by atom manipulation. *Angew. Chem. Int. Ed.* **59**, 22989–22993 (2020).
44. Geagea, E. et al. Collective radical oligomerisation induced by an STM tip on a silicon surface. *Nanoscale* **13**, 349–354 (2021).
45. Kawai, S. et al. Thermal control of sequential on-surface transformation of a hydrocarbon molecule on a copper surface. *Nat. Commun.* **7**, 12711 (2016).
46. Clair, S. & De Oteyza, D. G. Controlling a chemical coupling reaction on a surface: tools and strategies for on-surface synthesis. *Chem. Rev.* **119**, 4717–4776 (2019).
47. Piskun, I. et al. Covalent C–N bond formation through a surface catalyzed thermal cyclodehydrogenation. *J. Am. Chem. Soc.* **142**, 3696–3700 (2020).
48. Song, S. et al. Real-space imaging of a single-molecule monoradical reaction. *J. Am. Chem. Soc.* **142**, 13550–13557 (2020).
49. Ratera, I. & Veciana, J. Playing with organic radicals as building blocks for functional molecular materials. *Chem. Soc. Rev.* **41**, 303–349 (2012).
50. Zhou, X. et al. Steering surface reaction dynamics with a self-assembly strategy: Ullmann coupling on metal surfaces. *Angew. Chem. Int. Ed.* **56**, 12852–12856 (2017).
51. Nitzan, A. & Ratner, M. A. Electron transport in molecular wire junctions. *Science* **300**, 1384–1389 (2003).
52. Cheng, Z. et al. In situ formation of highly conducting covalent Au–C contacts for single-molecule junctions. *Nat. Nanotechnol.* **6**, 353–357 (2011).
53. Kiguchi, M. et al. Highly conductive molecular junctions based on direct binding of benzene to platinum electrodes. *Phys. Rev. Lett.* **101**, 046801 (2008).
54. Kaneko, S., Nakazumi, T. & Kiguchi, M. Fabrication of a well-defined single benzene molecule junction using Ag electrodes. *J. Phys. Chem. Lett.* **1**, 3520–3523 (2010).
55. Schneebeli, S. T. et al. Single-molecule conductance through multiple π–π-stacked benzene rings determined with direct electrode-to-benzene ring connections. *J. Am. Chem. Soc.* **133**, 2136–2139 (2011).
56. Martin, C. A. et al. Fullerene-based anchoring groups for molecular electronics. *J. Am. Chem. Soc.* **130**, 13198–13199 (2008).
57. Bulten, E. J. & Budding, H. A. The synthesis of small-ring monostannacycloalkanes. *J. Organomet. Chem.* **110**, 167–174 (1976).
58. Xu, B. & Tao, N. J. Measurement of single-molecule resistance by repeated formation of molecular junctions. *Science* **301**, 1221–1223 (2003).
59. Venkataraman, L. et al. Single-molecule circuits with well-defined molecular conductance. *Nano Lett.* **6**, 458–462 (2006).
60. Hybertsen, M. S. et al. Amine-linked single-molecule circuits: systematic trends across molecular. *J. Phys. Condens. Matter* **20**, 374115 (2008).
61. Olavarria-Contreras, I. J. et al. C–Au covalently bonded molecular junctions using nonprotected alkynyl anchoring groups. *J. Am. Chem. Soc.* **138**, 8465–8469 (2016).
62. Hong, W. et al. Trimethylsilyl-terminated oligo(phenylene ethynylene)s: an approach to single-molecule junctions with covalent Au–C σ-bonds. *J. Am. Chem. Soc.* **134**, 19425–19431 (2012).
63. Bennett, M. A., Bhargava, S. K., Hockless, D. C. R., Welling, L. L. & Willis, A. C. Dinuclear cycloaurated complexes containing bridging (2-diphenylphosphino) phenylphosphine and (2-diethylphosphino) phenylphosphine, $C_6H_4PR_2$ (R=Ph, Et). Carbon–carbon bond formation by reductive elimination at a gold(ii)-gold(ii) center. *J. Am. Chem. Soc.* **118**, 10469–10478 (1996).
64. Chen, W. & Widawsky, J. R. Highly conducting π-conjugated molecular junctions covalently bonded to gold electrodes. *J. Am. Chem. Soc.* **133**, 17160–17163 (2011).
65. Hines, T. et al. Controlling formation of single-molecule junctions by electrochemical reduction of diazonium terminal groups. *J. Am. Chem. Soc.* **135**, 3319–3322 (2013).
66. Peiris, C. R. et al. Metal–single-molecule–semiconductor junctions formed by a radical reaction bridging gold and silicon electrodes. *J. Am. Chem. Soc.* **141**, 14788–14797 (2019).
67. Pla-Vilanova, P. et al. The spontaneous formation of single-molecule junctions via terminal alkynes. *Nanotechnology* **26**, 381001 (2015).
68. Starr, R. L. et al. Gold–carbon contacts from oxidative addition of aryl iodides. *J. Am. Chem. Soc.* **142**, 7128–7133 (2020).
69. Bourissou, D., Guerret, O., Gabbaï, F. P. & Bertrand, G. Stable carbenes. *Chem. Rev.* **100**, 39–91 (2000).
70. Tulevski, G. S., Myers, M. B., Hybertsen, M. S., Steigerwald, M. L. & Nuckolls, C. Formation of catalytic metal-molecule contacts. *Science* **309**, 591–594 (2005).
71. Ren, F., Feldman, A. K., Carnes, M., Steigerwald, M. & Nuckolls, C. Polymer growth by functionalized ruthenium nanoparticles. *Macromolecules* **40**, 8151–8155 (2007).
72. Zhukhovitskiy, A. V., MacLeod, M. J. & Johnson, J. A. Carbene ligands in surface chemistry: from stabilization of discrete elemental allotropes to modification of nanoscale and bulk substrates. *Chem. Rev.* **115**, 11503–11532 (2015).

73. Zhukhovitskiy, A. V., Mavros, M. G., Van Voorhis, T. & Johnson, J. A. Addressable carbene anchors for gold surfaces. *J. Am. Chem. Soc.* **135**, 7418–7421 (2013).
74. Crudden, C. M. et al. Simple direct formation of self-assembled N-heterocyclic carbene monolayers on gold and their application in biosensing. *Nat. Commun.* **7**, 12654 (2016).
75. Ott, L. S., Cline, M. L., Deetlefs, M., Seddon, K. R. & Finke, R. G. Nanoclusters in ionic liquids: Evidence for N-heterocyclic carbene formation from imidazolium-based ionic liquids detected by ^{2}H NMR. *J. Am. Chem. Soc.* **127**, 5758–5759 (2005).
76. Hurst, E. C., Wilson, K., Fairlamb, I. J. S. & Chechik, V. N-Heterocyclic carbene coated metal nanoparticles. *New J. Chem.* **33**, 1837–1840 (2009).
77. Weidner, T. et al. NHC-based self-assembled monolayers on solid gold substrates. *Aust. J. Chem.* **64**, 1177–1179 (2011).
78. Crudden, C. M. et al. Ultra stable self-assembled monolayers of N-heterocyclic carbenes on gold. *Nat. Chem.* **6**, 409–414 (2014).
79. Wang, G. et al. Ballbot-type motion of N-heterocyclic carbenes on gold surfaces. *Nat. Chem.* **9**, 152–156 (2017).
80. Doud, E. A. et al. In situ formation of N-heterocyclic carbene-bound single-molecule junctions. *J. Am. Chem. Soc.* **140**, 8944–8949 (2018).
81. Gonell, S., Poyatos, M. & Peris, E. Triphenylene-based tris(N-heterocyclic carbene) ligand: unexpected catalytic benefits. *Angew. Chem. Int. Ed.* **52**, 7009–7013 (2013).
82. Capozzi, B. et al. Single-molecule diodes with high rectification ratios through environmental control. *Nat. Nanotechnol.* **10**, 522–527 (2015).
83. Lovat, G. et al. Room-temperature current blockade in atomically defined single-cluster junctions. *Nat. Nanotechnol.* **12**, 1050–1054 (2017).
84. Baghernejad, M. et al. Electrochemical control of single-molecule conductance by Fermi- level tuning and conjugation switching. *J. Am. Chem. Soc.* **136**, 17922–17925 (2014).
85. Darwish, N. et al. Observation of electrochemically controlled quantum interference in a single anthraquinone-based norbornylogous bridge molecule. *Angew. Chem. Int. Ed.* **51**, 3203–3206 (2012).
86. Brooke, R. J. et al. Single-molecule electrochemical transistor utilizing a nickel-pyridyl spinterface. *Nano Lett.* **15**, 275–280 (2015).
87. Mattei, M. et al. Tip-enhanced Raman voltammetry: coverage dependence and quantitative modeling. *Nano Lett.* **17**, 590–596 (2017).
88. Aragonès, A. C. et al. Electrostatic catalysis of a Diels–Alder reaction. *Nature* **531**, 88–91 (2016).
89. Dulić, D. et al. One-way optoelectronic switching of photochromic molecules on gold. *Phys. Rev. Lett.* **91**, 207402 (2003).
90. Jia, C. et al. Covalently bonded single-molecule junctions with stable and reversible photoswitched conductivity. *Science* **352**, 1443–1446 (2016).
91. Broman, S. L. et al. Dihydroazulene photoswitch operating in sequential tunneling regime: synthesis and single-molecule junction studies. *Adv. Funct. Mater.* **22**, 4249–4258 (2012).
92. Whalley, A. C., Steigerwald, M. L., Guo, X. & Nuckolls, C. Reversible switching in molecular electronic devices. *J. Am. Chem. Soc.* **129**, 12590–12591 (2007).
93. Kronemeijer, A. J. et al. Reversible conductance switching in molecular devices. *Adv. Mater.* **20**, 1467–1473 (2008).
94. Uchida, K., Yamanoi, Y., Yonezawa, T. & Nishihara, H. Reversible on/off conductance switching of single diarylethene immobilized on a silicon surface. *J. Am. Chem. Soc.* **133**, 9239–9241 (2011).
95. Tam, E. S. et al. Single-molecule conductance of pyridine-terminated dithienylethene switch molecules. *ACS Nano* **5**, 5115–5123 (2011).
96. Aradhya, S. V. et al. Dissecting contact mechanics from quantum interference in single-molecule junctions of stilbene derivatives. *Nano Lett.* **12**, 1643–1647 (2012).
97. Ikeda, M., Tanifuji, N., Yamaguchi, H. & Matsuda, K. Photoswitching of conductance of diarylethene-Au nanoparticle network. *Chem. Commun.* https://doi.org/10.1039/B617246F (2007).
98. Li, C. et al. Charge transport in single Au | alkanedithiol | Au junctions: coordination geometries and conformational degrees of freedom. *J. Am. Chem. Soc.* **130**, 318–326 (2008).
99. Kim, Y. et al. Conductance and vibrational states of single-molecule junctions controlled by mechanical stretching and material variation. *Phys. Rev. Lett.* **106**, 196804 (2011).
100. Li, L., Lo, W.-Y., Cai, Z., Zhang, N. & Yu, L. Proton-triggered switch based on a molecular transistor with edge-on gate. *Chem. Sci.* **7**, 3137–3141 (2016).
101. Meng, F. et al. Orthogonally modulated molecular transport junctions for resettable electronic logic gates. *Nat. Commun.* **5**, 3023 (2014).
102. Green, J. E. et al. A 160-kilobit molecular electronic memory patterned at 10^{11} bits per square centimetre. *Nature* **445**, 414–417 (2007).
103. Xu, B. Q., Li, X. L., Xiao, X. Y., Sakaguchi, H. & Tao, N. J. Electromechanical and conductance switching properties of single oligothiophene molecules. *Nano Lett.* **5**, 1491–1495 (2005).
104. Díez-Pérez, I. et al. Ambipolar transport in an electrochemically gated single-molecule field-effect transistor. *ACS Nano* **6**, 7044–7052 (2012).
105. He, J., Fu, Q., Lindsay, S., Ciszek, J. W. & Tour, J. M. Electrochemical origin of voltage-controlled molecular conductance switching. *J. Am. Chem. Soc.* **128**, 14828–14835 (2006).
106. Li, Z., Liu, Y., Mertens, S. F. L., Pobelov, I. V. & Wandlowski, T. From redox gating to quantized charging. *J. Am. Chem. Soc.* **132**, 8187–8193 (2010).
107. Janin, M., Ghilane, J. & Lacroix, J.-C. When electron transfer meets electron transport in redox-active molecular nanojunctions. *J. Am. Chem. Soc.* **135**, 2108–2111 (2013).
108. Yin, X. et al. A reversible single-molecule switch based on activated antiaromaticity. *Sci. Adv.* **3**, eaao2615 (2017).
109. Su, T. A., Li, H., Steigerwald, M. L., Venkataraman, L. & Nuckolls, C. Stereoelectronic switching in single-molecule junctions. *Nat. Chem.* **7**, 215–220 (2015).
110. Collier, C. P. et al. A [2]catenane-based solid state electronically reconfigurable switch. *Science* **289**, 1172–1175 (2000).
111. Kubatkin, S. et al. Single-electron transistor of a single organic molecule with access to several redox states. *Nature* **425**, 698–701 (2003).
112. Miyamachi, T. et al. Robust spin crossover and memristance across a single molecule. *Nat. Commun.* **3**, 938 (2012).
113. Aragonès, A. C. et al. Large conductance switching in a single-molecule device through room temperature spin-dependent transport. *Nano Lett.* **16**, 218–226 (2016).
114. Pasupathy, A. N. et al. The Kondo effect in the presence of ferromagnetism. *Science* **306**, 86–89 (2004).
115. Cho, W. J., Cho, Y., Min, S. K., Kim, W. Y. & Kim, K. S. Chromium porphyrin arrays as spintronic devices. *J. Am. Chem. Soc.* **133**, 9364–9369 (2011).
116. Feringa, B. L., Van Delden, R. A., Koumura, N. & Geertsema, E. M. Chiroptical molecular switches. *Chem. Rev.* **100**, 1789–1816 (2000).
117. Choudhury, J. & Semwal, S. Emergence of stimuli-controlled switchable bifunctional catalysts. *Synlett* **29**, 141–147 (2018).
118. Broichhagen, J., Frank, J. A. & Trauner, D. A roadmap to success in photopharmacology. *Acc. Chem. Res.* **48**, 1947–1960 (2015).
119. Zhang, N. et al. A single-molecular AND gate operated with two orthogonal switching mechanisms. *Adv. Mater.* **29**, 1701248 (2017).
120. Walkey, M. C. et al. Chemically and mechanically controlled single-molecule switches using spiropyrans. *ACS Appl. Mater. Interfaces* **11**, 36886–36894 (2019).
121. Xu, L., Izgorodina, E. I. & Coote, M. L. Ordered solvents and ionic liquids can be harnessed for electrostatic catalysis. *J. Am. Chem. Soc.* **142**, 12826–12833 (2020).
122. Rogers, F. J. M., Noble, B. B. & Coote, M. L. Computational optimization of alkoxyamine-based electrochemical methylation. *J. Phys. Chem. A* **124**, 6104–6110 (2020).
123. Dutta Dubey, K., Stuyver, T., Stuyver, T., Kalita, S. & Shaik, S. Solvent organization and rate regulation of a Menshutkin reaction by oriented external electric fields are revealed by combined MD and QM/MM calculations. *J. Am. Chem. Soc.* **142**, 9955–9965 (2020).
124. Meir, R., Chen, H., Lai, W. & Shaik, S. Oriented electric fields accelerate Diels–Alder reactions and control the *endo*/*exo* selectivity. *ChemPhysChem* **11**, 301–310 (2010).
125. Gryn'ova, G., Marshall, D. L., Blanksby, S. J. & Coote, M. L. Switching radical stability by pH-induced orbital conversion. *Nat. Chem.* **5**, 474–481 (2013).
126. Gryn'ova, G. & Coote, M. L. Origin and scope of long-range stabilizing interactions and associated SOMO–HOMO conversion in distonic radical anions. *J. Am. Chem. Soc.* **135**, 15392–15403 (2013).
127. Shaik, S., de Visser, S. P. & Kumar, D. External electric field will control the selectivity of enzymatic-like bond activations. *J. Am. Chem. Soc.* **126**, 11746–11749 (2004).
128. Fried, S. D., Bagchi, S., Boxer & Steven, G. Extreme electric fields power catalysis in the active site of ketosteroid isomerase. *Science* **346**, 1510–1514 (2014).
129. Welborn, V. V., Pestana, L. R. & Head-Gordon, T. Computational optimization of electric fields for better catalysis design. *Nat. Catal.* **1**, 649–655 (2018).
130. Che, F. et al. Elucidating the roles of electric fields in catalysis: a perspective. *ACS Catal.* **8**, 5153–5174 (2018).
131. Ciampi, S., Darwish, N., Aitken, H. M., Díez-Pérez, I. & Coote, M. L. Harnessing electrostatic catalysis in single molecule, electrochemical and chemical systems: a rapidly growing experimental tool box. *Chem. Soc. Rev.* **47**, 5146–5164 (2018).
132. Foroutan-Nejad, C. & Marek, R. Potential energy surface and binding energy in the presence of an external electric field: modulation of anion–π interactions for graphene-based receptors. *Phys. Chem. Chem. Phys.* **16**, 2508–2514 (2014).
133. Lau, V. M., Pfalzgra, W. C., Markland, T. E. & Kanan, M. W. Electrostatic control of regioselectivity in Au(i)-catalyzed hydroarylation. *J. Am. Chem. Soc.* **139**, 4035–4041 (2017).
134. Meyers, F., Marder, S. R., Pierce, B. M. & Brēdas, J. L. Electric field modulated nonlinear optical properties of donor–acceptor polyenes: sum-over-states investigation of the relationship between molecular polarizabilities (α, β, and γ) and bond length alternation. *J. Am. Chem. Soc.* **116**, 10703–10714 (1994).
135. Robertson, J. C., Coote, M. L. & Bissember, A. C. Synthetic applications of light, electricity, mechanical force and flow. *Nat. Rev. Chem.* **3**, 290–304 (2019).
136. Zang, Y. et al. Directing isomerization reactions of cumulenes with electric field. *Nat. Commun.* **10**, 4482 (2019).
137. Huang, X. et al. Electric field-induced selective catalysis of single-molecule reaction. *Sci. Adv.* **5**, eaaw3072 (2019).
138. Gross, L., Mohn, F., Moll, N., Liljeroth, P. & Meyer, G. The chemical structure of a molecule resolved by atomic force microscopy. *Science* **325**, 1110–1114 (2009).
139. Albrecht, F., Neu, M., Quest, C., Swart, I. & Repp, J. Formation and characterization of a molecule–metal–molecule bridge in real space. *J. Am. Chem. Soc.* **135**, 9200–9203 (2013).
140. Pavliček, N. et al. On-surface generation and imaging of arynes by atomic force microscopy. *Nat. Chem.* **7**, 623–628 (2015).
141. Schuler, B. et al. Reversible Bergman cyclization by atomic manipulation. *Nat. Chem.* **8**, 220–224 (2016).
142. de Oteyza, D. G. et al. Direct imaging of covalent bond structure in single-molecule chemical reactions. *Science* **340**, 1434–1438 (2013).
143. Pavlicek, N. & Gross, L. Generation, manipulation and characterization of molecules by atomic force microscopy. *Nat. Rev. Chem.* **1**, 0005 (2017).
144. Kaiser, K. et al. An sp-hybridized molecular carbon allotrope, cyclo[18]carbon. *Science* **365**, 1299–1301 (2019).
145. Zang, Y. et al. Electronically transparent Au–N bonds for molecular junctions. *J. Am. Chem. Soc.* **139**, 14845–14848 (2017).
146. Harun, M. K., Lyon, S. B. & Marsh, J. Formation and characterisation of thin phenolic amine-functional electropolymers on a mild steel substrate. *Prog. Org. Coat.* **52**, 246–252 (2005).
147. Leff, D. V., Brandt, L. & Heath, J. R. Synthesis and characterization of hydrophobic, organically-soluble gold nanocrystals functionalized with primary amines. *Langmuir* **12**, 4723–4730 (1996).
148. Adenier, A., Chehimi, M. M., Gallardo, I., Pinson, J. & Vilà, N. Electrochemical oxidation of aliphatic amines and their attachment to carbon and metal surfaces. *Langmuir* **20**, 8243–8253 (2004).
149. Bélanger, D. & Pinson, J. Electrografting: a powerful method for surface modification. *Chem. Soc. Rev.* **40**, 3995–4048 (2011).
150. Gallardo, I., Pinson, J. & Vilà, N. Spontaneous attachment of amines to carbon and metallic surfaces. *J. Phys. Chem. B* **110**, 19521–19529 (2006).
151. Xu, B., Zhou, L., Madix, R. J. & Friend, C. M. Highly selective acylation of dimethylamine mediated by oxygen atoms on metallic gold surfaces. *Angew. Chem. Int. Ed.* **49**, 394–398 (2010).

152. Venkataraman, L., Klare, J. E., Nuckolls, C., Hybertsen, M. S. & Steigerwald, M. L. Dependence of single-molecule junction conductance on molecular conformation. *Nature* **442**, 904–907 (2006).
153. Mishchenko, A. et al. Influence of conformation on conductance of biphenyl-dithiol single-molecule contacts. *Nano Lett.* **10**, 156–163 (2010).
154. Zang, Y. et al. In situ coupling of single molecules driven by gold-catalyzed electrooxidation. *Angew. Chem. Int. Ed.* **58**, 16008–16012 (2019).
155. Funes-Ardoiz, I. & Maseras, F. Oxidative coupling mechanisms: current state of understanding. *ACS Catal.* **8**, 1161–1172 (2018).
156. Liu, C., Zhang, H., Shi, W. & Lei, A. Bond formations between two nucleophiles: transition metal catalyzed oxidative cross-coupling reactions. *Chem. Rev.* **111**, 1780–1824 (2011).
157. Yan, M., Kawamata, Y. & Baran, P. S. Synthetic organic electrochemical methods since 2000: on the verge of a renaissance. *Chem. Rev.* **117**, 13230–13319 (2017).
158. Stamenkovic, V. R., Strmcnik, D., Lopes, P. P. & Markovic, N. M. Energy and fuels from electrochemical interfaces. *Nat. Mater.* **16**, 57–69 (2016).
159. She, Z. W. et al. Combining theory and experiment in electrocatalysis: Insights into materials design. *Science* **355**, eaad4998 (2017).
160. Jonsson, M., Lind, J., Eriksen, T. E. & Merényi, G. Redox and acidity properties of 4-substituted aniline radical cations in water. *J. Am. Chem. Soc.* **116**, 1423–1427 (1994).
161. Pavitt, A. S., Bylaska, E. J. & Tratnyek, P. G. Oxidation potentials of phenols and anilines: correlation analysis of electrochemical and theoretical values. *Environ. Sci. Process. Impacts* **19**, 339–349 (2017).
162. Merino, E. Synthesis of azobenzenes: the coloured pieces of molecular materials. *Chem. Soc. Rev.* **40**, 3835–3853 (2011).

Acknowledgements
This work was supported primarily by the NSF CHE-2023568 CCI Phase I: Center for Chemistry with Electric Fields. L.V. and X.R. acknowledge support from the NSF through the award CHE-1807654.

Author contributions
I.S. and R.L.S. contributed equally to this work, proposed the conceptual framework and wrote the first draft. All authors contributed to the discussion and writing of the Review.

Competing interests
The authors declare no competing interests.

Publisher's note
Springer Nature remains neutral with regard to jurisdictional claims in published maps and institutional affiliations.